

# High Efficiency Configuration Space Sampling – probing the distribution of available states

Paweł T. Jochym\* and Jan Łażewski

Institute of Nuclear Physics, Polish Academy of Sciences, Cracow, Poland

\* pawel.jochym@ifj.edu.pl

January 20, 2021

## 1 Abstract

Substantial acceleration of research and more efficient utilization of resources can be achieved in modeling investigated phenomena by identifying the limits of system’s accessible states instead of tracing the trajectory of its evolution. The proposed strategy uses the Metropolis-Hastings Monte-Carlo sampling of the configuration space probability distribution coupled with physically-motivated prior probability distribution. We demonstrate this general idea by presenting a high performance method of generating configurations for lattice dynamics and other computational solid state physics calculations corresponding to non-zero temperatures. In contrast to the methods based on molecular dynamics, where only a small fraction of obtained data is consumed, the proposed scheme is distinguished by a considerably higher, reaching even 80%, acceptance ratio.

---

## Contents

1	Introduction	1
2	General idea of HECSS	2
3	Sampling of probability distribution	4
4	Convergence of derived quantities	7
5	Conclusions	8
	References	8

---

## 2 1 Introduction

Every system can be successfully studied by methodical observation of its behaviour for a long enough time. However, especially for slowly changing characteristics, this could take proverbial eons. On the other hand, some elementary knowledge of possible features and existing constrains allows one to limit available states of the studied system and determine the probability distribution of these states in the configuration space. As a result, the system can be modeled based on its probable configurations. To illustrate this idea, we present its application to studies of vibrational properties of solids.

10 A number of problems in solid state physics connected with lattice dynamics can be  
11 effectively addressed with inter-atomic potential models constructed using data obtained  
12 from quantum mechanical calculations (e.g. Density Functional Theory – DFT). Probably  
13 the simplest of such models is harmonic approximation developed by Born and von Kármán  
14 at the beginning of the 20th century [1–3]. Over the years multiple increasingly more  
15 sophisticated models have been developed: Quasi-Harmonic approximation (QHA) [4],  
16 Temperature-Dependent Effective Potential [5–7], Self-Consistent Phonons (SCPH) [8] or  
17 Parlinski’s approach [9], to name just a few. All the above mentioned schemes share  
18 common feature – they need an appropriate set of data to build a model of inter-atomic  
19 potential which is essential for this type of methods. The data set should correspond to the  
20 system at thermal equilibrium or other physical state. It is usually comprised of atomic  
21 positions as well as resulting energies and forces calculated with some quantum mechanical  
22 (e.g. DFT) or even effective potential method.

23 Presently, molecular dynamics is often used to investigate systems at non-zero tem-  
24 perature in thermal equilibrium. This is done either directly – by analysis of the MD  
25 trajectory – or as a source of configurations for building the mentioned effective models of  
26 the inter-atomic potential to be used in further analysis (e.g. with programs like ALAM-  
27 ODE [10, 11] or TDEP [7]). Both cases involve a very costly stage of running long MD  
28 calculations [12]. Since uncorrelated configurations from different parts of the phase space  
29 are required, they are generated by appropriate spacing of the sampling points over the  
30 computed trajectory or even by performing multiple independent MD runs. At the end  
31 only a small fraction of calculated configurations is used (typically 1-10%). Therefore, us-  
32 ing MD in this context is exceedingly wasteful. This makes it not only very expensive but  
33 also useless for larger and more complicated systems (of hundreds or more atoms), where  
34 even static, single-point DFT calculations are challenging. In such cases running a 30000  
35 steps MD becomes prohibitively expensive and impractical.

36 In this work we propose a new, High Efficiency Configuration Space Sampling (HECSS)  
37 method for modelling systems in non-zero temperature, including non-harmonic effects,  
38 without using MD trajectory. We also indicate its possible application to some additional  
39 cases like disordered systems or large, complicated systems.

## 40 2 General idea of HECSS

41 To reproduce the thermal equilibrium in the system, independent configurations of dis-  
42 placements consistent with a desired non-zero temperature should be selected. Having  
43 any initial approximations for the lattice dynamics of the system (e.g. standard har-  
44 monic approach [2, 4, 13]) one can estimate temperature-dependent atomic mean-square-  
45 displacements (MSD) from a small set of force-displacement relations. Using these MSD  
46 data as a first approximation, the atomic displacements with normal distribution around  
47 equilibrium positions can be easily generated. There is, however, a subtle issue around  
48 displacements generated this way – they are *uncorrelated* between atoms, while in reality  
49 atomic displacements are correlated at least for their close neighbours. For example, it  
50 is easy to see that a simultaneous out-of-phase movement of neighboring atoms towards  
51 or away from each other will generate larger changes in energy than a synchronous in-  
52 phase movement of the same atoms. The former configuration should be represented with  
53 lower probability than the later, instead of equal probability present in the above simplistic  
54 scheme. Thus, while the static configurations generation may be a correct direction in gen-  
55 eral, such a naive approach is not sufficient. One can see that some additional mechanism  
56 is required to adjust probability distribution of generated samples in order to accurately

57 reproduce configurations drawn from thermodynamic equilibrium ensemble. Classical sta-  
 58 tistical mechanics points to such a scheme for selection of configurations representing a  
 59 system in thermal equilibrium.

60 The general form of the equipartition theorem says that a generalized virial for any  
 61 phase space coordinate (i.e. generalized coordinate or momentum) is proportional to tem-  
 62 perature when it is averaged over the whole ensemble:

$$\left\langle x_m \frac{\partial H}{\partial x_n} \right\rangle = \delta_{mn} k_B T. \quad (1)$$

63 If we assume ergodicity of the system, the ensemble average may be replaced with time  
 64 average. For momenta this leads to the average kinetic energy per degree of freedom being  
 65 equal to  $k_B T/2$  and provides the kinetic definition of temperature. However, the relation  
 66 holds also for derivatives of Hamiltonian with respect to positions. Considering relation (1)  
 67 for some atomic displacement  $q$  from the equilibrium configuration, and assuming the  
 68 potential energy depends only on position, we can write position-dependent part of the  
 69 Hamiltonian (i.e the potential energy  $E_p(q)$ ) as a Taylor's expansion with respect to the  
 70 atomic displacement  $q$  from the equilibrium configuration:

$$E_p(q) = \sum_{n=2}^{\infty} C_n q^n, \quad (2)$$

71 where the expansion coefficients  $C_n$  are, in general, functions of all remaining coordinates  
 72 (displacements). The equipartition theorem (1) now takes the form:

$$k_B T = \left\langle q \sum_{n=2}^{\infty} n C_n q^{n-1} \right\rangle = \sum_{n=2}^{\infty} n C_n \langle q^n \rangle \quad (3)$$

73 and if we write  $n$  as  $(n-2) + 2$  and divide both sides by 2 we get:

$$\langle E_p(q) \rangle = \frac{k_B T}{2} - \sum_{n=3}^{\infty} \frac{n-2}{2} C_n \langle q^n \rangle, \quad (4)$$

74 which is similar to the kinetic energy counterpart except for an additional term generated by  
 75 the anharmonic part of the potential and defined by the third and higher central moments of  
 76 the probability distribution of the displacements. If we can assume that the second term of  
 77 the Eq. 4 is small in comparison with  $k_B T$ , we get a formula for the average potential energy  
 78 of the system. Note that for harmonic systems the second part vanishes. For anharmonic  
 79 systems omission of higher terms in Eq. 4 will provide first-order approximation of the  
 80 mean potential energy. Only experience can tell us how good this approximation is and  
 81 how wide its applicability range is. However, one should note that substantial higher-order  
 82 terms are present only in parts of the formula connected with strongly anharmonic modes.  
 83 Furthermore, for every atom in centro-symmetric position all odd-power moments vanish  
 84 and the first non-zero moment is the fourth one. Finally, the formula for the potential  
 85 energy of the whole system contains similar terms for all modes. Judging by extremely  
 86 high efficiency of harmonic approximation for crystal lattice dynamics, we can expect that  
 87 this averaging will make proposed approximation effective for a wide range of systems.

88 To sum up, MD provides a representation of the system with the properly distributed  
 89 kinetic energy. For a single particle it is a Maxwell-Boltzmann distribution. By virtue  
 90 of the central limit theorem (CLT) [14, 15], if we increase the number of particles we will  
 91 approach at infinity (i.e. in the thermodynamical limit) a Gaussian distribution with the  
 92 same average (the same mean) and the variance which is scaled as inverse number of

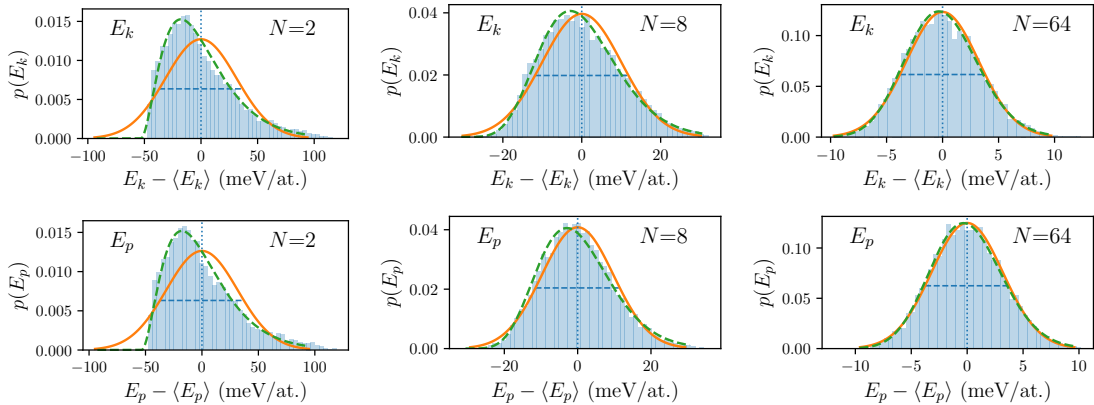


Figure 1: Probability distribution for single atom kinetic (upper) and potential (lower) energies averaged over  $N = 2, 8$  and  $64$  randomly selected atoms. Solid orange lines show fitted normal distributions while dashed green lines show  $\chi^2$  distribution for  $3N$  degrees of freedom fitted to kinetic energy histograms. Data derived from the MD trajectory.

93 particles. As we can see for kinetic energy the relation is very simple whereas for the  
 94 potential energy we have a quantity approximately close to temperature if the system is  
 95 not too far from a harmonic one. Nevertheless, we do not know, in general, the form  
 96 of the distribution of the potential energy. That constitutes substantial difficulty, which  
 97 fortunately can be overcome by application of the CLT to calculate distribution of potential  
 98 energy.

99 The CLT states that for any reasonable probability distribution, the distribution of the  
 100 mean of the sample of the independent random variable drawn from it tends to the normal  
 101 distribution with the same mean and variance scaled by the square root of the number  
 102 of samples. The *reasonable* class is very broad here, certainly containing all physically  
 103 interesting cases by virtue of requiring a finite variance and a well-defined mean. Thus,  
 104 for potential energy per degree of freedom we can expect the probability distribution con-  
 105 verging to the normal distribution:

$$\lim_{N \rightarrow \infty} p(E_p) = \mathcal{N}(\langle E_p \rangle, \sigma / \sqrt{3N}). \quad (5)$$

106 As shown above, one can approximate the  $\langle E_p \rangle$  with the first term of Eq. 4 and the only  
 107 unknown parameter in this formula is the variance of the distribution. Note that above  
 108 expression is *independent* from the particular shape of the potential energy probability  
 109 distribution for the single degree of freedom except of its mean  $\langle E_p \rangle$  and variance  $\sigma$ .

110 However, we need to consider that the Eq. 5 is true *asymptotically*. At this point we need  
 111 to decide if this relation has any practical use for *finite*, and preferably not too large,  $N$ .  
 112 The common wisdom in statistical community states that for  $N$  above  $\approx 50$  the distribution  
 113 of the average is practically indistinguishable from the true normal distribution, and even  
 114 for smaller  $N$ , if the starting distribution is not too wild, the convergence is usually very  
 115 quick.

### 116 3 Sampling of probability distribution

117 To verify if this “folk wisdom” holds true for the typical kinetic and potential distributions  
 118 we have checked this hypothesis against actual MD data of a typical system. This test does  
 119 not require high-accuracy forces and energies but demands ability to efficiently calculate

120 moderately sized systems (e.g. 1000 atoms). Thus, instead of using DFT as a source of  
 121 energies/forces we have used effective potential model of the cubic 3C-SiC crystal. We have  
 122 used LAMMPS [16] implementation of the potential with parameters derived in [17,18] and  
 123 the NVT-MD implemented in ASAP3 module of the Atomistic Simulation Environment  
 124 (ASE) [19]. High performance of this implementation allowed for  $5 \cdot 10^4$  time steps (of 1 fs  
 125 length) runs of the  $5 \times 5 \times 5$  supercell (1000 atoms) to be executed on a single server in  
 126 just a few hours.

127 The kinetic and potential energy probabil-  
 128 ity distributions extracted from MD runs of  
 129 systems of 2, 8 and 64 atoms (i.e. 6, 24, 192  
 130 degrees of freedom) are presented in Fig. 1. At  
 131 this stage we are interested in the speed of conver-  
 132 gence of the probability distribution, and  
 133 this experiment shows that for typical distri-  
 134 butions present in crystals the convergence is  
 135 quite quick. Already at the  $N_{DOF} = 24$  (i.e. 8  
 136 atoms) the deviation from the normal distribu-  
 137 tion is barely noticeable and at  $N_{DOF} = 192$   
 138 (i.e. 64 atoms) it is indeed hardly visible. And  
 139 that seems to hold true equally well for distri-  
 140 butions of the kinetic and potential energy.

141 This simple example demonstrates that for  
 142 our practical purposes we can expect the central  
 143 limit theorem in application to energy distri-  
 144 bution in crystals to hold above  $\approx 30$  de-  
 145 grees of freedom, for both the kinetic and po-  
 146 tential energies. This means that we can apply  
 147 this approach even for very moderately sized  
 148 systems of 10-20 or more atoms.

149 The energy distributions in Fig. 1, derived from the MD runs mentioned above, show  
 150 clearly Gaussian distributions for both the kinetic and potential energies even for  $N_{DOF} \approx$   
 151 25 degrees of freedom. Furthermore, the variance of these distributions plotted against the  
 152 system's size and shown in Fig. 2 follows closely CLT prediction in Eq. 5. And this holds  
 153 true for parts of a larger system (blue circles in Fig. 2) as well as for the whole smaller  
 154 crystals (squares and triangles in Fig. 2). The dispersion of small systems' data in Fig. 2  
 155 is due to large temperature fluctuations in small sets of particles.

156 Thus, we have checked that, at least in our test case, the convergence to thermody-  
 157 namic and CLT limits required by the Eqs 4 and 5 is quick enough to be useful in practical  
 158 calculations for systems of just tens of atoms. The main problem now is that there is  
 159 no direct access to potential energy and there is no way to invert relation from positions  
 160 to potential energy – even in principle since the relation is many-to-one. Our goal here  
 161 is to reproduce the potential energy distribution described by Eq. 5 and present in MD  
 162 data by intelligently sampling the configuration space of the system – since this is the  
 163 only input we can directly specify. Fortunately, computational statistics provides multiple  
 164 algorithms dedicated to the task of sampling of indirectly specified probability distribu-  
 165 tions. In particular, the Metropolis-Hastings Monte Carlo [20] seems well suited to our  
 166 purposes. To use it effectively we need to generate a prior distribution which covers the do-  
 167 main and, preferably, is fairly close to the target distribution. Obviously, we are unable to  
 168 generate configurations corresponding to the distribution from Eq. 5 but we can use physi-  
 169 cally motivated approximation. We propose to approximate displacements of atoms in the

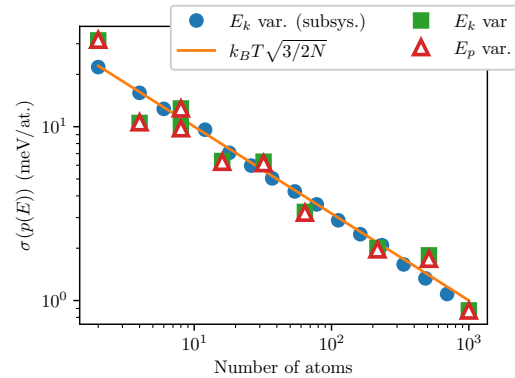


Figure 2: Variance of the energy distribution as a function of system size compared with prediction of the central limit theorem (orange line). Results for different numbers of randomly chosen coordinates of  $5 \times 5 \times 5$  system (blue circles) were put together with variance of both the kinetic (green squares) and potential (red triangles) energies of smaller systems (defined in the text).

170 system by Gaussian probability distribution with variance tuned to the temperature and  
 171 to the resulting energy. Our HECSS software package provides the Metropolis-Hastings  
 172 implementation together with a tuned prior probability distribution generator. The tun-  
 173 ing algorithm adjusts the variance of the atomic displacement distribution in each step:  
 174  $\sigma_{n+1} = (1 + s(E_p(x_n)))\sigma_n$ , according to the modified logistic sigmoid function:

$$s(E_p) = \delta \left( \frac{2}{1 + e^{-(E_p - E_0)/(w \cdot \sigma_{E_p})}} - 1 \right), \quad (6)$$

175 where  $\sigma_{E_p} = k_B T \sqrt{3/2N}$  is the variance of  
 176 the target potential energy distribution (5)  
 177 and  $\delta \approx 0.005 - 0.02$  is a small tuning pa-  
 178 rameter controlling the speed of the variance  
 179 adjustment, while  $w \approx 3$  controls the width  
 180 of the prior distribution. Both parameters  
 181 have substantial practical importance – they  
 182 influence the effectiveness of the procedure –  
 183 but play no fundamental role in the algorithm.  
 184 Changing these parameters to the unsuitable  
 185 values leads only to slower convergence of the  
 186 procedure, since the Metropolis-Hastings algo-  
 187 rithm is guaranteed to asymptotically produce  
 188 the target distribution for any non-vanishing  
 189 prior distribution. A good selection of the  
 190 prior distribution means getting higher than  
 191 50% (in practice even above 80%) acceptance  
 192 ratio instead of a few percent or even less if the prior distribution is very far from the target.  
 193 The prior distribution we are proposing here is already of similar shape to the target one,  
 194 thus it results in several additional samples at the start of the procedure to properly tune  
 195 the width parameter – if it was not set correctly.

196 The typical good relationship between  
 197 prior and target distribution as well as the  
 198 sampling produced by the proposed algorithm  
 199 is illustrated in Fig. 3. Furthermore, the near-  
 200 independent drawing of each step in the algo-  
 201 rithm means that each sample from the pro-  
 202 duced set is potentially usable. Therefore, the  
 203 burn-in period may be reduced to just a few  
 204 samples required for tuning of the prior dis-  
 205 tribution parameters. The only source of pos-  
 206 sible correlations between samples in consec-  
 207 utive steps is the change in variance of the prior  
 208 distribution, which is tuned after each step ac-  
 209 cording to the sigmoid function (defined by  
 210 Eq. 6). This is a very weak correlation since  
 211 the variance is not supposed to change by more  
 212 than  $\delta \approx 0.5 - 2\%$ . What is more, these pa-  
 213 rameters are independent from the size of the  
 214 system and their values are not critical. The variance of the prior distribution, which is  
 215 self-tuning, should be estimated with 20% accuracy in order for the burn-in period to be re-  
 216 duced to just one or two samples. Thus, the initial tuning may be performed using a small

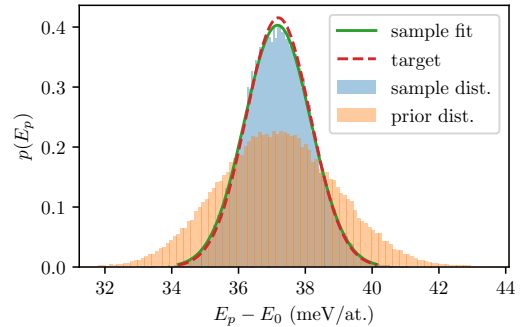


Figure 3: Prior energy probability distribution (orange filling) versus target distribution (blue filling). The lines indicate target distribution (red dashed line) and Gaussian distribution fitted to generated sample (green solid line).

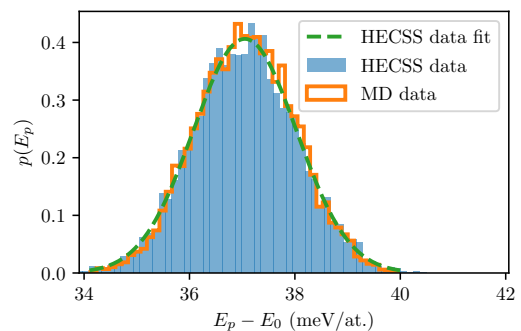


Figure 4: Probability distribution of potential energy per atom generated with HECSS scheme (blue shape) versus distribution extracted from the MD trajectory (orange contour). The dashed line indicates normal distribution fitted to HECSS sample.

217 supercell or even a primitive unit cell – depending on the system – by just recording the  
 218 self-tuning trajectory of the algorithm and adapting initial parameters of the production  
 219 run accordingly.

220 The end result of these algorithms is a series of samples (i.e. configurations) which  
 221 reproduce expected probability distribution (5) of potential energy for the system in ther-  
 222 mal equilibrium at the target temperature. The comparison between the potential energy  
 223 probability distribution in the samples generated by HECSS and extracted from the MD  
 224 run is depicted in Fig. 4.

## 225 4 Convergence of derived quantities

226 The results presented above demonstrate that  
 227 it is possible to effectively generate samples  
 228 with potential energy distributions consistent  
 229 with the data from the MD trajectories. The  
 230 remaining, much more difficult, question is  
 231 whether these samplings indeed provide an  
 232 appropriate representation of the system in  
 233 thermal equilibrium at a given temperature.  
 234 This issue may be tested in various ways. In  
 235 this work we propose to check if the potential  
 236 model built basing on the HECSS-generated  
 237 displacement-force data provides phonon fre-  
 238 quencies and lifetimes consistent with those  
 239 derived from the MD trajectory data.

240 Therefore, we have compared the results  
 241 obtained from the calculations of 3C-SiC crys-  
 242 tal with LAMPPS potential used in the previ-  
 243 ous section. The samples obtained by both  
 244 methods (i.e. MD and HECSS) have been  
 245 used to build force constants matrices for the  
 246 material with ALAMODE program. Both  
 247 second- and third-order force constants have  
 248 been determined based on different number  
 249 of samples. The resulting phonon frequencies  
 250 and lifetimes are presented in Fig. 5 and Fig. 6,  
 251 respectively. These findings demonstrate not  
 252 only high-level of consistency between both  
 253 data sets and models, but also similar conver-  
 254 gence characteristics between both methods.

255 It is important to note that HECSS-  
 256 generated data sets consist of first  $N$  gener-  
 257 ated samples (after initial burn-in period of 3  
 258 samples), not the  $N$  samples selected from the  
 259 larger set, as it is done with MD trajectory.

260 Obviously, if one were forced to run as many steps of HECSS algorithm as time steps, of  
 261 the MD trajectory the whole effort would be pointless. It is evident that the results of both  
 262 approaches are very similar, despite a large difference in necessary computational effort –  
 263 which provides a clear justification for future application of the presented method to the

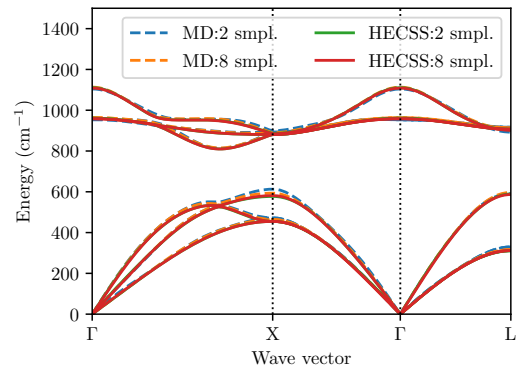


Figure 5: Consistency and convergence of phonon frequencies in 3C-SiC crystal determined with harmonic model derived from MD (dashed lines) and HECSS (solid lines) data.

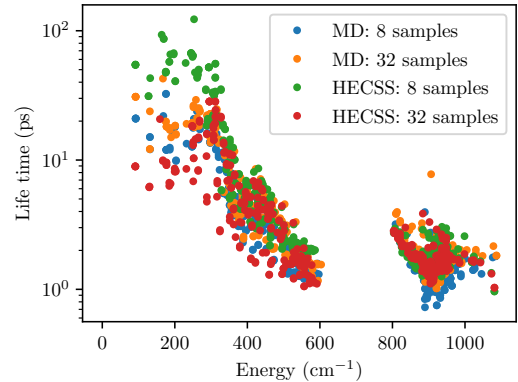


Figure 6: Consistency and convergence of 3C-SiC phonon lifetimes derived with third order model based on MD (blue and orange) and HECSS (green and red) generated data.

264 much more expensive DFT-based variant of the potential energy calculation.

## 265 5 Conclusions

266 We have introduced a new high efficiency configuration space sampling (HECSS) scheme  
267 as an alternative for application of Molecular Dynamics as a source of configurations rep-  
268 resenting systems at non-zero temperatures. The results presented above demonstrate  
269 potential of the proposed HECSS method to generate faithful configuration samplings for  
270 systems in thermal equilibrium, which can be used to investigate anharmonic effects present  
271 in crystalline solids. It is worth noting that this method is not limited to crystals or to  
272 only geometric degrees of freedom. In principle, it is possible to extend its applicability  
273 to magnetic degrees of freedom or disordered systems. Furthermore, due to its inherent  
274 ability to provide  $3 \times$  number-of-atoms force-displacement data points per configuration, it  
275 reduces number of DFT calculations required for simple harmonic model determination.  
276 This reduction is much more pronounced in higher-order models, where number of inde-  
277 pendent variables is usually large. It should also be emphasized that the generated samples  
278 are drawn from the physically meaningful distribution and not from the non-physical, sin-  
279 gle axis displacements. This difference may become important if there is any substantial  
280 anharmonicity in the system, which couples degrees of freedom.

## 281 Acknowledgments

282 The authors would like to express their gratitude to Krzysztof Parlinski, Przemysław  
283 Piekarz, Andrzej M. Oleś, and Małgorzata Sternik for very inspiring and fruitful discus-  
284 sions. This work was partially supported by National Science Centre (NCN, Poland) under  
285 grant UMO-2017/25/B/ST3/02586.

## 286 References

- 287 [1] M. Born and T. V. Kármán, *Über Schwingungen in Raumgittern. (German) [On*  
288 *vibrations in space lattices]*, *Physikalische Zeitschrift* **13**(8), 297 (1912).
- 289 [2] A. A. Maradudin, *Theory of Lattice Dynamics in the Harmonic Approximation*, New  
290 York (1963).
- 291 [3] M. Born and K. Huang, *Dynamical Theory of Crystal Lattices*, Oxford University  
292 Press (1988).
- 293 [4] B. Fultz, *Vibrational thermodynamics of materials*, *Progress in Materials Science*  
294 **55**(4), 247 (2010), doi:10.1016/j.pmatsci.2009.05.002.
- 295 [5] O. Hellman, I. A. Abrikosov and S. I. Simak, *Lattice dynamics of anhar-*  
296 *monic solids from first principles*, *Physical Review B* **84**(18), 180301 (2011),  
297 doi:10.1103/PhysRevB.84.180301.
- 298 [6] O. Hellman, P. Steneteg, I. A. Abrikosov and S. I. Simak, *Temperature dependent*  
299 *effective potential method for accurate free energy calculations of solids*, *Physical*  
300 *Review B* **87**(10), 104111 (2013), doi:10.1103/PhysRevB.87.104111.

- 301 [7] O. Hellman and I. A. Abrikosov, *Temperature-dependent effective third-order inter-*  
302 *atomic force constants from first principles*, Physical Review B **88**(14), 144301 (2013),  
303 doi:10.1103/PhysRevB.88.144301.
- 304 [8] T. Tadano and S. Tsuneyuki, *Self-consistent phonon calculations of lattice dynamical*  
305 *properties in cubic SrTiO<sub>3</sub> with first-principles anharmonic force constants*, Physical  
306 Review B **92**(5), 054301 (2015), doi:10.1103/PhysRevB.92.054301.
- 307 [9] K. Parlinski, *Ab initio determination of anharmonic phonon peaks* **98**(5), 054305  
308 (2018), doi:10.1103/PhysRevB.98.054305.
- 309 [10] Y. Oba, T. Tadano, R. Akashi and S. Tsuneyuki, *First-principles study of phonon*  
310 *anharmonicity and negative thermal expansion in ScF<sub>3</sub>*, Physical Review Materials  
311 **3**(3), 033601 (2019), doi:10.1103/PhysRevMaterials.3.033601.
- 312 [11] T. Tadano, Y. Gohda and S. Tsuneyuki, *Anharmonic force constants extracted*  
313 *from first-principles molecular dynamics: Applications to heat transfer simulations*,  
314 Journal of Physics: Condensed Matter **26**(22), 225402 (2014), doi:10.1088/0953-  
315 8984/26/22/225402.
- 316 [12] N. Shulumba, O. Hellman and A. J. Minnich, *Intrinsic localized mode and*  
317 *low thermal conductivity of PbSe*, Physical Review B **95**(1), 014302 (2017),  
318 doi:10.1103/PhysRevB.95.014302.
- 319 [13] K. Parlinski, Z. Q. Li and Y. Kawazoe, *First-Principles Determination of*  
320 *the Soft Mode in Cubic ZrO<sub>2</sub>*, Physical Review Letters **78**(21), 4063 (1997),  
321 doi:10.1103/PhysRevLett.78.4063.
- 322 [14] G. Pólya, *Über den zentralen Grenzwertsatz der Wahrscheinlichkeitsrech-*  
323 *nung und das Momentenproblem*, Mathematische Zeitschrift **8**(3), 171 (1920),  
324 doi:10.1007/BF01206525.
- 325 [15] D. C. Montgomery and G. C. Runger, *Applied Statistics and Probability for Engineers*,  
326 Wiley, New York (2003).
- 327 [16] S. Plimpton and B. Hendrickson, *A new parallel method for molecular dynamics*  
328 *simulation of macromolecular systems*, Journal of Computational Chemistry **17**(3),  
329 326 (1996), doi:10.1002/(SICI)1096-987X(199602)17:3<326::AID-JCC7>3.0.CO;2-X.
- 330 [17] P. Erhart and K. Albe, *Analytical potential for atomistic simulations of sil-*  
331 *icon, carbon, and silicon carbide*, Physical Review B **71**(3), 035211 (2005),  
332 doi:10.1103/PhysRevB.71.035211.
- 333 [18] E. B. Tadmor, R. S. Elliott, J. P. Sethna, R. E. Miller and C. A. Becker, *The potential*  
334 *of atomistic simulations and the knowledgebase of interatomic models*, JOM **63**(7), 17  
335 (2011), doi:10.1007/s11837-011-0102-6.
- 336 [19] A. H. Larsen, J. J. Mortensen, J. Blomqvist, I. E. Castelli, R. Christensen, M. Duřak,  
337 J. Friis, M. N. Groves, B. Hammer, C. Hargus, E. D. Hermes, P. C. Jennings *et al.*, *The*  
338 *atomic simulation environment—a Python library for working with atoms*, Journal of  
339 Physics: Condensed Matter **29**(27), 273002 (2017), doi:10.1088/1361-648X/aa680e.
- 340 [20] W. K. Hastings, *Monte Carlo sampling methods using Markov chains and their appli-*  
341 *cations*, Biometrika **57**(1), 97 (1970), doi:10.1093/biomet/57.1.97.